Chinese Journal of Aeronautics, (2017), 30(1): 235–248

Chinese Society of Aeronautics and Astronautics
& Beihang University

Chinese Journal of Aeronautics

cja@buaa.edu.cn
www.sciencedirect.com

Discretized Miller approach to assess effects on boundary layer ingestion induced distortion

Esteban Valencia [a,*], Víctor Hidalgo [a], Devaiah Nalianda [b], Laskaridis Panagiotis [b], Riti Singh [b]

[a] *Departamento de Ingeniería Mecánica, Facultad de Ingeniería Mecánica, Escuela Politécnica Nacional, Ladron de Guevara E11-253, Quito 17-01-2759, Ecuador*
[b] *School of Engineering, Cranfield University, Bedford MK43 0AL, United Kingdom*

Received 19 November 2015; revised 27 June 2016; accepted 19 October 2016
Available online 21 December 2016

KEYWORDS

BLI;
Correlations;
Distortion;
Embedded propulsors;
Empirical;
Mean-line analysis;
Turbomachinery

Abstract The performance of propulsion configurations with boundary layer ingestion (BLI) is affected to a large extent by the level of distortion in the inlet flow field. Through flow methods and parallel compressor have been used in the past to calculate the effects of this aerodynamic integration issue on the fan performance; however high-fidelity through flow methods are computationally expensive, which limits their use at preliminary design stage. On the other hand, parallel compressor has been developed to assess only circumferential distortion. This paper introduces a discretized semi-empirical performance method, which uses empirical correlations for blade and performance calculations. This tool discretizes the inlet region in radial and circumferential directions enabling the assessment of deterioration in fan performance caused by the combined effect of both distortion patterns. This paper initially studies the accuracy and suitability of the semi-empirical discretized method by comparing its predictions with CFD and experimental data for a baseline case working under distorted and undistorted conditions. Then a test case is examined, which corresponds to the propulsor fan of a distributed propulsion system with BLI. The results obtained from the validation study show a good agreement with the experimental and CFD results under design point conditions.
© 2016 Chinese Society of Aeronautics and Astronautics. Production and hosting by Elsevier Ltd. This is an open access article under the CC BY-NC-ND license (http://creativecommons.org/licenses/by-nc-nd/4.0/).

1. Introduction

The performance of axial fans under distorted conditions has been studied extensively in the past. Different approaches and tools such as through flow methods,[1] semi-empirical correlations,[2] and fan map based methods (parallel compressor[3]) have been utilized to assess their performance. It has been found that even though through flow methods such as streamline curvature[4,5] and CFD can predict fan performance with

* Corresponding author. Tel.: +593 99 664 5322.
E-mail address: esteban.valencia@epn.edu.ec (E. Valencia).
Peer review under responsibility of Editorial Committee of CJA.

Production and hosting by Elsevier

http://dx.doi.org/10.1016/j.cja.2016.12.005
1000-9361 © 2016 Chinese Society of Aeronautics and Astronautics. Production and hosting by Elsevier Ltd.
This is an open access article under the CC BY-NC-ND license (http://creativecommons.org/licenses/by-nc-nd/4.0/).

Nomenclature

i	incidence, β_{LE} - β'_{LE}
C	absolute flow velocity, m/s
P	total pressure, Pa
p	static pressure, Pa
T	total temperature, K
t	static temperature, K
$()_f$	fan property
OD	off design conditions
BLI	boundary layer ingestion
ε	deflection, β_{LE} - β_{TE}
β	relative air angle
V	relative velocity, m/s
U	tangential velocity, m/s
C_a	axial velocity
α	absolute air angle
δ	deviation angle, β_{TE} - β'_{TE}
ω	total loss coefficient
ω_p	profile loss coefficient
ω_{sec}	secondary loss coefficient
ω_{sw}	shock wave loss coefficient
ΔP_{ideal}	ideal total pressure increment, Pa
ΔP_{real}	real total pressure increment, Pa
P'_{LE}	ideal total pressure at leading edge, Pa
P_{LE}	total pressure at leading edge, Pa
$\bar{\omega}$	average total loss coefficient
$\omega_{p,\ par}$	parametric profile loss coefficient
$\omega_{ew,\ par}$	parametric end wall loss coefficient
V_{LE}	relative velocity at leading edge
V_{TE}	relative velocity at trailing edge
β_{TE}	relative air angle at trailing edge
β'_{TE}	relative blade angle at trailing edge
h	blade height, m
c	blade chord, m
h/c	blade aspect ratio
r	radius, m
y^+	dimensionless distance of the node from the wall
k–ε	k-epsilon turbulence model
k–ω	k-ω turbulence model
H	H grid type
C	C grid type
O	O grid type
ATM	automatic topology and meshing
P_{BL}	total pressure in the boundary layer region at propulsor intake
Ma_{BL}	Mach number in the boundary layer region at propulsor intake
Ma_∞	Mach number at free stream conditions
P_∞	total pressure at free stream conditions
TeDP	turboelectric distributed propulsion
y	perpendicular distance from the wall, m
C_{cl}	airframe length
R_c	Reynolds number
ψ	flow coefficient
CFD	computational fluid dynamics
BL	boundary layer
DM	discretized Miller
DC_{120}	distortion coefficient for 120°
θ	angular position, rad or °
ml	minimum loss
$\dot{m}$	mass flow
r_{rt}	root to tip ratio
FPR	fan pressure ratio
V_{tip}	tip velocity, m/s
η_f	fan efficiency
DP	design point
NB	number of blades
r_t	tip radius, m
r_r	root radius, m
$()_1$	properties at rotor entry
$()_2$	properties at stator entry
TSFC	thrust specific fuel consumption

higher accuracy than other methods, they also require more resources in terms of computational power and time. For boundary layer ingestion (BLI) systems, streamline curvature and parallel compressor have been combined in order to assess circumferential and radial distortion.[4] In the case of CFD, this tool enables the assessment of the fan performance radially and circumferentially, and for this reason CFD has also been utilized for the assessment of BLI distortion problems. This approach has been preferred for cases where the detailed geometry is known and accuracy is paramount. In this study, CFD has been used to compare some results obtained under uniform conditions with the discretized Miller approach. Some experimental test-rigs have been set for the assessment of BLI type distortion; however testing engines or in this case fans are expensive and the cost increases with advanced engine technology and designs. Furthermore, the cost of the energy required for each run and the possibility of damaging the tested equipment increase the difficulty of carrying out these procedures. Jerez et al.[1] experimentally studied the validation of a CFD model for a fan working under distortion. Redmond[6] described a test-rig and experimental results for BLI type distortion; however in this latter case, the uncertainties achieved are large and it is difficult to assess the real benefits of BLI.

At the preliminary design stage when the detailed geometry of a system/component is still undefined and several configurations have to be tested, reducing requirements of computational resources becomes imperative.

Due to excessive simulation times, these methods have also been found unsuitable in cases where full annular simulation is required and circumferential distortion is present (such as in boundary layer ingesting systems[7–9]). These reasons, therefore, make methods such as the parallel compressor[3] more attractive for preliminary design at design point. However, this method has its limitations, as it only enables to assess circumferential distortion. Hence it may be considered to have limited accuracy in the case of BLI systems where a combination of circumferential and radial distortion of flow is observed.

This paper addresses this limitation of the method and proposes a novel approach to overcome it. Using a semi-empirical approach, the proposed method essentially utilizes empirical

data for the blade and performance calculations. Further by discretizing the inlet region in circumferential and radial directions, the proposed approach takes into account the combined effects of the distortion patterns on fan performance calculation.

In order to verify the approach and ensure that the set of empirical correlations predicts the fan performance accurately, a series of validation test cases are undertaken. The first stage of the validation is undertaken against data available in the study of Osborn et al.[10] for the NASA axial flow fan stage 53 utilizing experimental data and CFD under similar operating conditions. It commences with the assessment of fan performance at design point under various off-design operating conditions, assuming a uniform inlet flow field. The next stage of validation examines the performance of the fan under distorted conditions. As no published data is available for the performance of the NASA axial flow fan stage 53, the data available for the NASA axial flow fan stage 67[1] is considered. The validation studies under uniform and distorted conditions are then followed by assessment of the fan performance assuming boundary layer ingestion, which is similar to conditions faced by a propulsor fan unit in a distributed propulsion system with BLI.[11,12] The operating conditions and propulsion system configuration for this final phase of validation is adapted from a previous parametric optimization study,[9] using the airframe design and cruise conditions of the NASA N3-X aircraft concept.[11]

Hierarchy of distortion methods

Fig. 1 shows the distortion methods that have been utilized for the assessment of BLI induced distortion. To illustrate where they are implemented in the propulsion system analysis, the input data and propulsor modules have been included in this diagram. As observed in this figure, the parametric method which was utilized by Valencia et al.[9] is the most basic approach where the fan performance characteristics are assumed. The other two methods assess the fan performance characteristics based on the fan face flow properties. This enables to relate the inlet flow characteristics with the propulsor performance.

2. Methodology

This section describes the methodology used to develop the discretized Miller approach. As the discretized Miller approach is based on the mean-line design and semi-empirical performance approaches, the first part of this section describes the conventional mean-line approach and the empirical correlations utilized for fan performance analysis, while the second part explains the discretized Miller approach. In order to carry out the fan performance calculation, a computer program (MATLAB platform) is developed.

The discretized Miller approach comprises several subroutines which follow a process as shown in Fig. 2. The input variables (in Fig. 2) are set by the inlet flow properties, fan geometric characteristics and fan operating conditions (as summarized in Table 1). The collected input data is used by the blade design subroutine, where the mean-line design approach allows defining the fan annular section and the air angles along the blade span.[13]

The blade design module is not necessary if the geometry is known, as the air angles and other parameters can be defined. The incorporation of the blade design module enables us to make the method independent of the fan geometry for the cases where this is unknown. This is an important feature for preliminary design of distributed propulsion systems, as different propulsor arrangements and hence fan configurations need to be tested. However, it is important to note that the

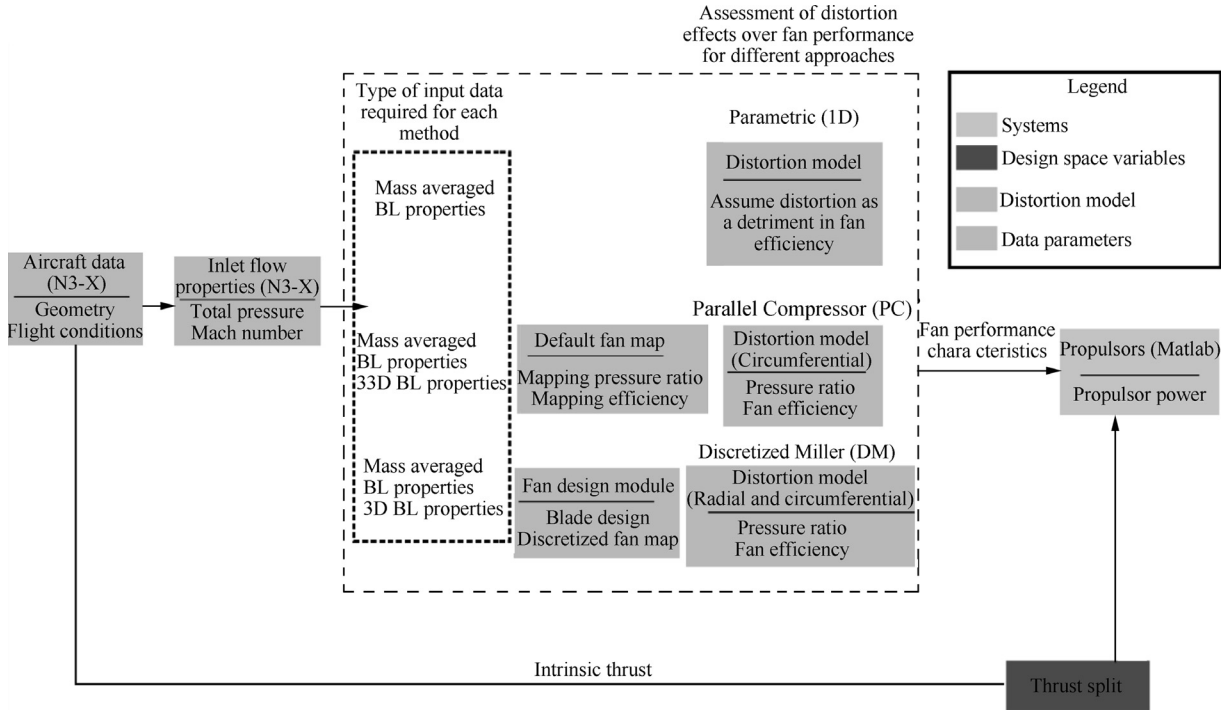

Fig. 1 Road map of distortion models.

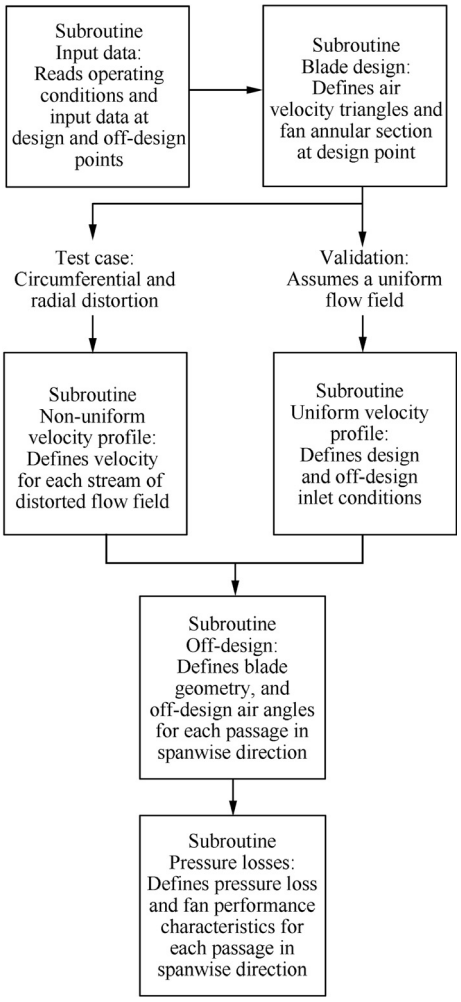

Fig. 2 Structure of fan performance program.

Table 1 Operating conditions and characteristics of fan 53 at design point.

Parameter	Value
Mass flow (kg/s)	32.65
Pressure ratio	1.35
Average inlet Mach number	0.57
Average inlet total pressure (kPa)	101.4
Average inlet total temperature (K)	288.2
Tip velocity v_{tip} (m/s)	302.8
Tip radius r_t (m)	0.254
Root to tip ratio r_{rt}	0.52
Clearance to chord ratio ε/c	0.01
Blade height to chord ratio midspan h/c	2.86
Pitch to chord ratio midspan s/c	0.70
Thickness to chord ratio midspan t/c	0.007

generation of the blade geometry following the method described in the next section (free vortex design) is basic and hence it will present discrepancy with the actual blade design. This aspect will reduce the accuracy of the method when the blade design module is utilized. The effects of using the actual and designed geometry will be examined later.

2.1. Mean-line design method

The mean-line method is a design approach, which uses the Euler equations and velocity triangles to calculate the air exit angles. These angles and empirical correlations for blade geometry and pressure losses allow us to calculate the fan performance. The blade arrangement studied in this work comprises a rotor and stator. A schematic representation of the fan stage is shown in Fig. 3.

For the calculation of the air exit angles, a free vortex condition and a constant axial velocity through the fan assembly are assumed. These assumptions allow simplification of the model at an expense of loss in accuracy (Section 3.1.2). Since the method to calculate the pitch to chord ratio shown in the study of Saravanamuttoo et al.[13] presents some discrepancies with the actual pitch to chord ratio of the fan examined, this parameter was assumed the same as the reported one in the work of Osborn et al.[10] for the validation studies. The blade geometry in the proposed method is determined using Carter's rule[2] for deviation angle δ. This approach was preferred over the Miller's[14] definition due to its simplicity and better prediction capability for the uniform case. For the non-uniform cases, the deviation angle, calculated as a function of the stagger and camber angles through empirical charts, is based on the methodology as described by Howell[15] and Miller.[14] This parameter then allows determining the minimum loss (ml), optimum stall and choke incidence angles. The loss coefficient calculation in the method follows the approach as described in the work of Howell[15], Miller[14] and White[16] and uses the sets of empirical correlations as summarized in Table 2.

The loss coefficient definition used in the fan performance calculation is given by Eq. (1), and is based on studies conducted by Howell[15], Miller[14] and Osborn.[10] The total loss coefficient is given by

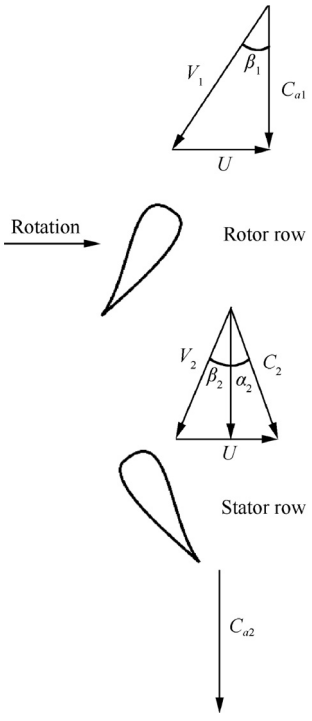

Fig. 3 Fan assembly used in propulsor unit of TeDP system.[6]

Table 2 Empirical approaches examined in this paper.

Item	Model			
	Set 1	Set 2	Set 3	Set 4[a]
$\bar{\omega}_{ml}$	Miller[14]	Howell[15]	Miller[14]	Miller[14]
δ OD	Miller[14]	Howell[15]	Miller[14]	Miller[14]
$\bar{\omega}$OD	Miller[14]	Howell[15]	–	Miller[14]
ω_{ew}	–	–	Wright[17]	Wright[17]
ω_{p}	–	–	Wright[17]	Wright[17]
ω_{sw}	–	–	Schwenk[18]	Schwenk[18]

[a] This case utilizes the approaches in Refs. 14, 17, 18 depending on the blade span section.

$$\omega = \frac{\Delta P_{ideal} - \Delta P_{real}}{P'_{LE} - P_{LE}} = \omega_p - \omega_{sec} \quad (1)$$

where ω_p and ω_{sec} stands for profile and secondary losses respectively. The secondary losses implemented in the model correspond to the end wall and shock wave effects. The ideal static pressure increment is calculated based on the assumption of constant relative total pressure across the rotor or constant total pressure for the case of the stator. As the fan assembly for the test case presents one stage and is expected to operate at low pressure ratio, the density variation and blockage effects across the blade arrangement are neglected.[13] These assumptions essentially simplify the model by enabling the use of incompressible flow equations. These equations can be used to calculate the static pressure increment, which for the case of constant axial speed is equal to the total pressure increment in the absolute frame of reference. This latter parameter together with the total loss coefficient is then used to determine the isentropic efficiency.[1] In the case of multi-stage configurations and high pressure ratios, the aforementioned assumptions reduce the accuracy of the method to a large extent. This is observed in the validation studies, and is discussed in the results section. A synthesized algorithm for the fan performance calculation encompassing the uniform and distorted flow cases is shown in Fig. 4.

2.2. Discretization Miller approach

In order to assess the radial and circumferential effects of ingesting a distorted flow field on fan performance, the mean-line design as previously described is modified. This modification uniformly discretizes the inlet rotor area into a number of blade passages and radial stations.

After establishing the blade design with the mean-line approach, the inlet area is discretized in a number of streams. Fig. 5 shows a schematic representation of the fan face flow properties for uniform and distorted cases and the discretization of the areas for each configuration. As observed, the model discretizes in the circumferential region based on the number of blade passages, whilst for the spanwise blade direction (radial) the number of streams is a user's input. In order to define an optimal set of values for this latter parameter, several

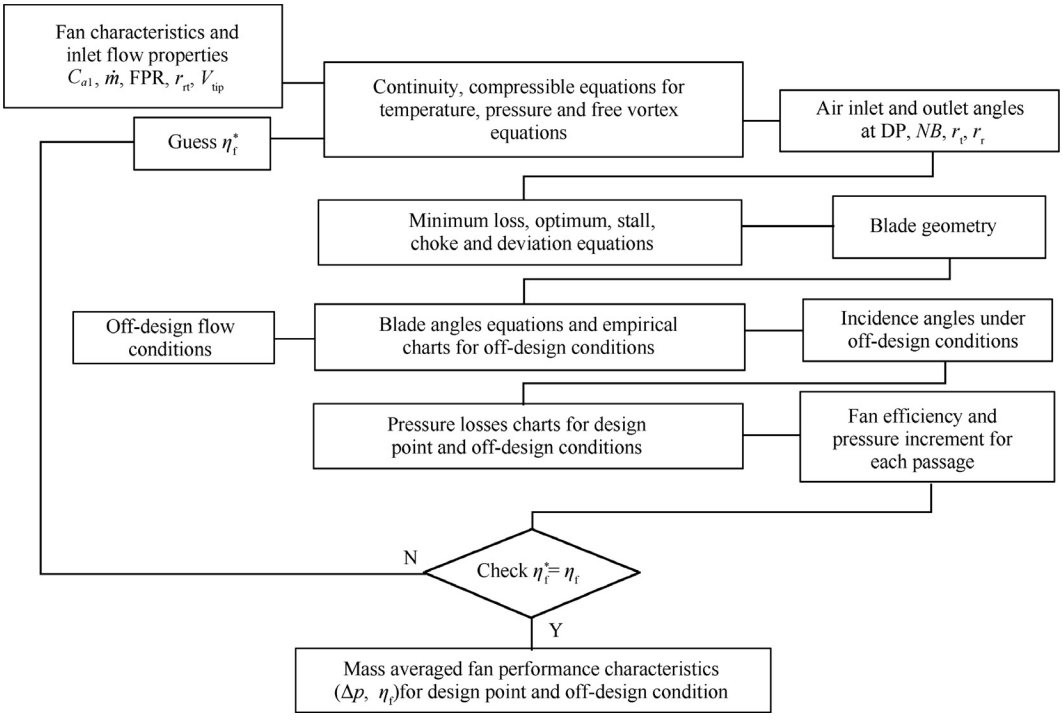

Fig. 4 Algorithm used for calculation of fan performance characteristics.

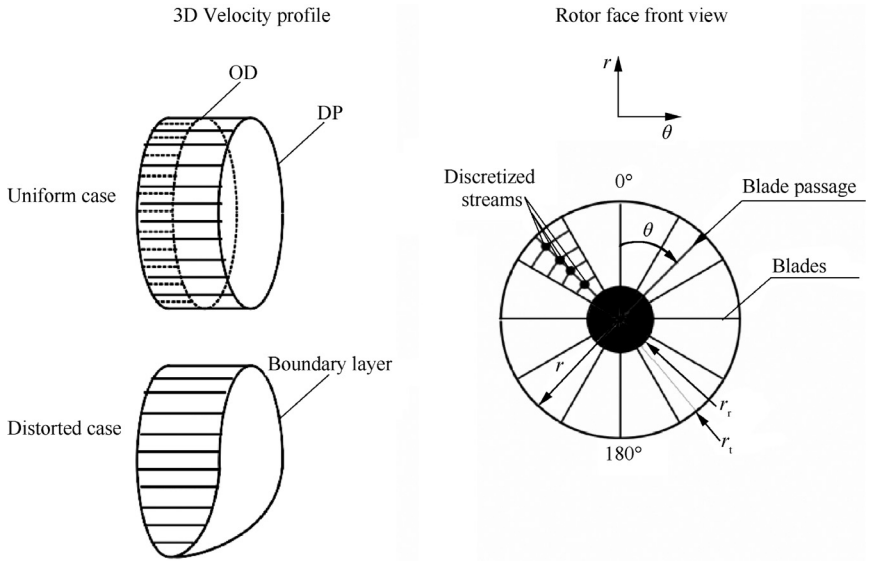

Fig. 5 Discretized fan area and three-dimensional velocity profiles for uniform and distorted cases. The angles in this analysis are accounted as shown on the right side of the figure.

cases are run and based on the accuracy needed and the computational resources this variable is defined. Although the present model is not computationally expensive compared with higher-fidelity tools such as CFD, the iterative calculation required can substantially increase the computational time. For instance, an increment in 5 streams in the spanwise direction would mean 150 points for a 30 blade passage case and hence the iterative calculation within the matrix arrangement would need to run for 150 times more. The parametric nature of the model and semi-empirical correlations for losses constrain up to certain extent the accuracy improvements and hence it is found in the present study that more than 10 streams do not enhance the trends obtained. Therefore, a range of discretized streams in the spanwise direction between 5 and 10 is found appropriate. To show better in detail how the trends of the flow performance are captured by the model, 10 streams have been selected in this work from hub to tip.

For each discretized stream, the air exit angle can be calculated in function of the speed triangles. This then enables the calculation of stall/choke angles and minimum loss for each stream in the discretized area, analogously to the mean-line approach.[15,19] The flow and blade characteristics at each position are then used to calculate their empirical losses utilizing different semi-empirical approaches based on compressor performance. Table 2 describes the semi-empirical approaches investigated in this work. The definition of the loss coefficient for each discretized stream using the aforementioned correlations allows us to calculate the stagnation pressure losses through the blade passage and hence the static pressure increments and fan efficiency for each stream. The matrix of values obtained by using the discretized model enables us to calculate the three-dimensional flow behavior across the fan.

Since the aim of this model is to be implemented in the parametric assessment of the propulsion performance of BLI systems,[9] the data obtained from the fan performance matrix is parametrized using the mass averaged values for static pressure increment and efficiency. These values then are used in the propulsion performance module as shown in Fig. 1.

It is pertinent for the reader to note that in this analysis the discretized area at the rotor face is considered constant till the stator exit. It is also important to note that as the empirical correlations cited by Schwenk and Lewis[18] and Wright and Miller[17] are developed for mean-line analysis, the variables in their definitions are not a function of the blade span and angular position. For the discretized Miller analysis undertaken in this study, the same expressions are used whilst angular and radial positions are taken into account. The loss coefficient definitions for profile and end wall losses in the discretized model are

$$\omega_{\mathrm{p}}(r,\theta) = \frac{\omega_{\mathrm{p,par}}(r,\theta)}{0.5 * \left(\frac{V_{\mathrm{LE}(r,\theta)}}{V_{\mathrm{TE}(r,\theta)}}\right)^2 \cos(\beta_{\mathrm{TE}(r,\theta)})} \tag{2}$$

$$\bar{\omega}_{\mathrm{ew}}(r,\theta) = \frac{\omega_{\mathrm{ew\,par}}(r,\theta)}{0.5 * \left(\frac{V_{\mathrm{LE}(r,\theta)}}{V_{\mathrm{TE}(r,\theta)}}\right)^2 h/c} \tag{3}$$

where ω_{par} (for end wall and profile losses) corresponds to the total loss parameter and depends on the diffusion factor.[17] Similar to equations for calculating loss coefficients, the diffusion factors are also calculated as a function of the position in the flow. It is clarified that in Eqs. (2) and (3) the radius r is defined by the number of stations along the blade span and the angular position θ is defined by the number of blade passages. For the uniform flow case, as there is no circumferential distortion, assessment of one blade passage is adequate. It is also important to note that the blade aspect ratio h/c is assumed constant at any span and circumferential location in Eq. (3). This assumption is observed to cause some discrepancies between the calculated and experimental values (Fig. 9). The shock wave loss coefficient is determined analogously to the profile and end wall loss coefficients. This means that the supersonic turning angle, relative inlet Mach number and peak suction surface Mach number[18] are defined for the radial and circumferential stations which are previously mentioned.

Because of the complexity of the flow in hub and tip regions, the empirical correlations presented by Wright and Miller[17] have certain discrepancies compared with the experimental data. In order to improve the prediction capability of the loss models in these regions, different sets of correlations are assessed and compared. In the case of the stator, the loss coefficient model presented by Miller[14] predicts with good accuracy the loss coefficients in all blade regions.

The complexity of the flow makes it difficult to capture the effect of the radial and circumferential distortion interactions between the discrete streams using empirical correlations and basic fan geometries, and therefore these have been usually studied with high-fidelity methods using detailed fan designs.[1,6] As the developed model aims to be simple and accurate enough for preliminary design, these interactions are neglected.

2.3. Model validation

To examine the accuracy of the discretized Miller approach, a baseline case which ingests a uniform flow field is studied. As discussed earlier, for the validation study under uniform conditions, the NASA axial flow fan stage 53[10] operating at similar pressure ratios as the test case is selected. For the validation under distorted conditions, CFD studies are carried out and comparisons are made with data available for NASA axial flow fan stage 67.[1]

Uniform inlet flow field is assumed for the baseline case, and hence the radial fluctuations in the flow field are neglected. The uniform velocity profile used for this case is based on the mass averaged flow properties under the test conditions for the NASA axial flow fan stage 53.[10] Table 1 lists some of the flow and fan characteristics.

2.3.1. CFD approach

In order to assess the balance between complexity demanded and accuracy provided using a high-fidelity approach, a CFD simulation is carried out to assess the fan performance. The results from this simulation then have been compared with the predictions of the discretized Miller approach. For this, the NASA axial flow fan stage 53 and a commercially available turbo-machinery performance analysis tool (ANSYS CFX)[20] are utilized. The CFD study is carried out for the uniform case using the flow and component characteristics reported by Osborn.[10]

The CFD analysis of the NASA axial flow fan stage 53 is carried out using total pressure and static pressure as inlet and outlet boundary conditions respectively. This approach is selected as it offers a reduced time for convergence and its results are found to be close to the experimental data. The values used for these boundary conditions at design point are described in Table 3.

Table 3 Boundary conditions at design point for ANSYS/CFD model under uniform conditions.

Station	P^b (kPa)	T^b (K)	P^a (kPa)
Inlet	101.4	288.2	–
Outlet	–	–	112.5

[a] Static characteristics.
[b] Total characteristics.

It is important to mention that during the simulation the solution cannot converge when this starts from the design point conditions (Table 3). This is because if the downstream static pressure is highly enough, the intense flow separation will cause high instability and impede the solution to converge. The method applied to solve the problem is to start simulation with relatively low back static pressure till initial convergence is achieved, and then increase it gradually by manipulating the outlet boundary condition.

(1) Meshing

For the creation of the 3D model, the program ANSYS bladegen and the data from report[10] have been used. The blade model was then implemented in ANSYS turbogrid for meshing. ATM Optimized Mesh Topology has been selected due to its capacity of facilitating the creation of the high-quality mesh. Fig. 6 presents the meshes of rotor and stator generated according to default ATM setting. Tip-Clearance was set at 0.4% of the blade height.

To refine the mesh depending on the turbulence model, different levels of mesh refinement near the wall (blade, hub and shroud) have been considered. y^+ is the dimensionless distance of the node from the wall. This value should be refined consistently in order to resolve properly the viscous sub-layer. This study considers a y^+ value of 40 for the k-ε model and $y^+ < 2$ for the k-ω model. In order to have a good accuracy in the boundary layer region at hub and blade tip, the k-ω turbulence model was chosen.

(2) Grid independence study

The accuracy and precision of the simulation depend largely upon the mesh type and size. An adequate mesh should present a good compromise between simulation accuracy and computational time. A large mesh could present accurate results, but at the same time be highly expensive in computational resources.

The quality of the mesh relies heavily on the grid type (H, C or O). In this case, as it is a preliminary study, the ATM Mesh Type in Turbogrid presents good qualities as it delivers an optimized mesh structure divided according to the curvature of the blade (Fig. 6). This simplifies the mesh independence study to mesh size study. For this purpose, four mesh sizes have been investigated as shown in Table 4. They present approximately the same refinement for rotor and stator; however the presence of tip clearance for the rotor case contributes to a larger number of elements for the rotor mesh.

The key parameters used for mesh-independence study are the spanwise distribution of pressure ratio, temperature ratio and the averaged stage efficiency. For space reasons, here only the results obtained for the stage efficiency are shown. Fig. 7 shows how the mesh size increment improves the accuracy of

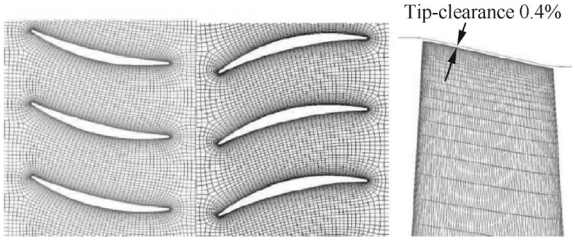

Fig. 6 Rotor and stator grids at midspan.[21]

Table 4 Distribution of grid elements in rotor and stator domains for different mesh sizes.[21]

Mesh	Rotor	Stator	Total
1	170920	100232	271152
2	225055	122692	347747
3	304517	163676	468193
4	421893	195422	617315

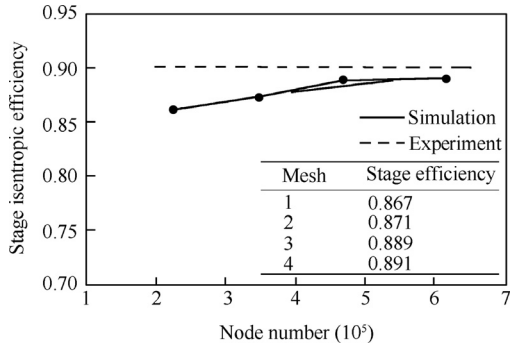

Fig. 7 Mesh size influence on isentropic efficiency.[21]

the results. However it is observed that the substantial improvement is obtained in the refinement from Mesh 1 to Mesh 3, whilst from Mesh 3 to Mesh 4 the improvement is less and the computational time is much longer. The good compromise between accuracy and computational time presented by Mesh 3 is the reason for it to be implemented in this CFD study.

The computational domain is shown in Fig. 8 and this reproduces the rotor and stator components. In order to ensure a uniform static pressure under the exit boundary condition, the exit stator component is assumed to have a length of three times the rotor radius.

2.3.2. Case studied: BLI configuration

The N3-X NASA aircraft concept is selected as the baseline architecture for the test case as it was designed to incorporate the turboelectric distributed propulsion system (TeDP) with boundary layer ingestion. As this work focuses on the fan performance assessment under distorted flow, the design point conditions and airframe configuration are assumed to be the same as those of the N3-X.[9,11] Table 5 summarizes the design

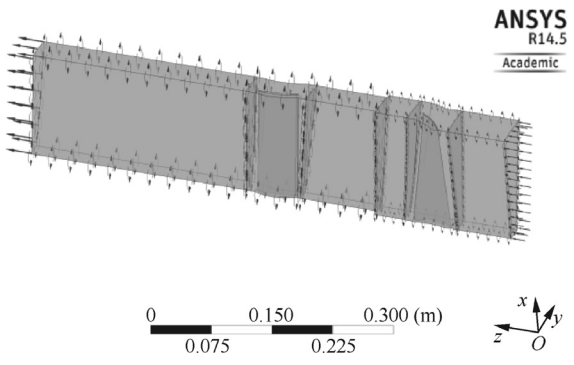

Fig. 8 CFD domain for uniform case.[21]

Table 5 Operating conditions at design point for BLI case.

Parameter	Value
Intrinsic thrust at cruise (12192m) (N)	73952.6
Thrust split	95%
Mach number at cruise	0.84
Number of propulsors	15
Propulsor mass flow (kg/s)	55.36
Pressure ratio	1.25
Fan face Mach number	0.6 (Uniform)
Inlet total pressure (kPa)	29.67 (Uniform)
Fan face Mach number[a]	0.5 (Distorted)
Inlet total pressure (kPa)[a]	28.87 (Distorted)
Inlet total temperature (K)	244.9
Tip velocity (m/s)	244.2[7]
Tip radius r_t (m)	0.6519

Notes: The remaining blade geometric properties are the same as those of the fan assembly 53.
[a] These properties correspond to the mass averaged values.

point conditions and fan design characteristics utilized for this study.

In order to calculate the flow properties at fan face, several assumptions are made. First, it is assumed that the inlet duct produces a drop in total pressure of 2%; second, the gradient of the total pressure and Mach number profiles remains the same until the fan face. To define the Mach number profile at fan face for the distorted case, an average Mach number of 0.5 is assumed. Based on this, the inlet Mach number profile is scaled up. The propulsor inlet total pressure and Mach number profiles are defined as a function of height and calculated using Eqs. (5) and (4) respectively.

$$Ma_{BL} = Ma_{\infty}\left(\frac{y}{0.371c_{cl}/Re_{cl}^{1/5}}\right)^{1/11} - 0.14 \tag{4}$$

$$P_{BL} = P_{\infty}\left(\frac{y}{0.371c_{cl}/Re_{cl}^{1/5}}\right)^{1/15} - 0.075 \tag{5}$$

where c_{cl} and Re_{cl} are the airframe length and Reynolds number respectively.

It is important to note that this study aims to assess the performance of a propulsor fan primarily designed for uniform conditions, but under the effects of distortion due to BLI. Under this premise, the distorted case starts with the design of the fan assuming the ingestion of uniform flow, which will not be the case in reality. However, this has been considered primarily to enable the assessment of fan performance and consequent deterioration, when a distorted flow field is ingested. After the fan geometry for the uniform flow is defined, the distorted condition is then assessed as a particular off-design case, where the flow properties vary in radial and circumferential locations.

In the test case, the flow coefficient ($\psi = C_a/U$) varies in radial and circumferential directions (depending on the three-dimensional axial velocity profile at the rotor inlet station, as observed in Fig. 5, due to the non-uniform axial velocity (C_a) that the ingested boundary layer presents. Therefore in this case, each discrete stream works under different operating conditions. For this reason, in this case, all the blade passages are assessed and then a radial and circumferential mass

average is used to define the average pressure ratio and fan stage efficiency.

3. Results and discussion

In this section, the results and discussion for the validation studies and the case studied (BLI configuration) are demonstrated.

3.1. Uniform case

The experimental data for the NASA axial flow fan stage 53 is used to select the most accurate set of empirical correlations for the loss coefficient. The selected set is then used to validate the discretized Miller approach.

3.1.1. Empirical correlations for loss coefficients

Since the loss prediction models have been developed for mean-line analysis, it is necessary to assess their suitability when they are used at different blade span locations. In this study, the loss prediction models described in Table 2 are investigated. In this table, Sets 1, 2 and 3 correspond to the approaches presented by Miller[14], Howell[15] and Wright and Miller.[17]

Howell's work[15] is one of the earliest studies regarding the effect of losses on turbomachinery performance. For this approach, the total loss coefficient is determined directly from charts presented in his work.[15] This aspect makes its implementation simple, nevertheless it does not enable assessing the effects of contributors to the total loss coefficient such as profile, end wall, shockwaves, and others. Another important work is presented by Miller[14] and it focuses on the off-design performance of turbomachinery and analogously to Howell, it introduces semi-empirical charts in order to calculate the off-design performance. However, this work presents the same problem as Howell's approach, as it only enables one to calculate the total loss coefficient. For this reason, Set 1 and Set 2 in Table 2 do not require the calculation of the loss contributors. In order to improve the performance prediction, Wright and Miller[17] and Miller[14] developed a model based on the individual source of losses in compressor performance and hence this approach allows one to individually calculate end wall, profile and shock wave losses. Fig. 9 collects the loss coefficient prediction using all the loss approaches aforementioned, which are described in Table 2.

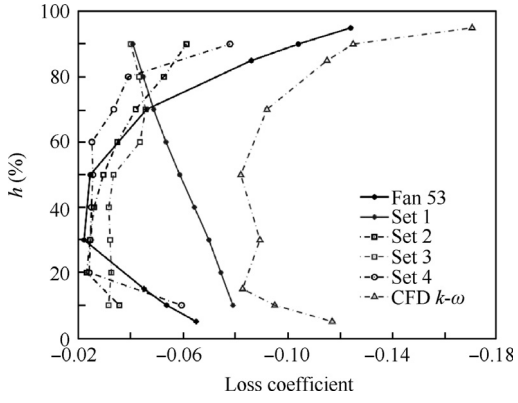

Fig. 9 Loss coefficients according to different empirical correlations.

As it is observed that depending on the region on the blade (root, mid and tip), some approaches are able to provide better predictions than others, a loss model that uses a suitable and best approach for each blade region is assessed. This approach is denominated Set 4 (Table 2) and it uses, for the tip region of the blade, the end wall and shock wave losses predicted by combining methods described by Wright and Miller[17] and those defined by the conventional Miller approach.[14] For the root and mid regions, the losses are predicted using methods described by Wright and Miller[17] and Miller[14] respectively. As Set 4 demonstrates the best results, it will be used in further analysis. This selected approach is from this point onwards referred to as the discretized Miller (DM) approach.

3.1.2. Stage performance of NASA's rotor 53

In this section, the stage performance of the NASA's fan 53 is assessed with the discretized Miller approach. This validation is only carried out for the uniform case.

(1) Case studied using report data

To illustrate the effects of some assumptions, such as uniform inlet velocity, free vortex design (including blade design module) and constant axial velocity through the fan assembly, on the predictions of the discretized Miller approach, a case that neglects these assumptions and takes these data from the report[10] is examined. Fig. 10 shows the fan performance characteristics when the actual data (from report) is used.

Fig. 10 shows that the discretized Miller approach captures the trend of the pressure increment and values of isentropic efficiency. It is observed that Set 4 of empirical correlations predicts the loss coefficients and isentropic efficiencies along the blade span with good accuracy. There are only some discrepancies in the tip and hub region, which can be attributed to the basic loss coefficient models and the uniform discretizing step utilized, and make the accurate assessment of the flow in these regions difficult. In the case of the pressure increment, an offset between the experimental and calculated values is observed, which can be attributed to the assumption of incompressible flow through the stage.

(2) Case studied using blade design module and constant velocity assumption

Fig. 10 shows the isentropic fan efficiency and pressure increment in a meridional section for the uniform case using the blade design module and the assumptions of constant axial speed and negligible radial distortion. As observed in Fig. 10, the implementation of the aforementioned assumptions produces a larger offset in the values predicted. Since the geometry predicted by free vortex and the blade angles are affected mainly in the tip and hub regions, it can be deduced that the increment in the gap in the midspan region is mainly produced by the assumption of constant velocity through the fan assembly. The experimental data[10] shows that there is certain difference in the axial velocities after the rotor, and if this is considered as in Fig. 10 (designed), the static pressure increment which is directly related to these velocities would match the experimental results better.

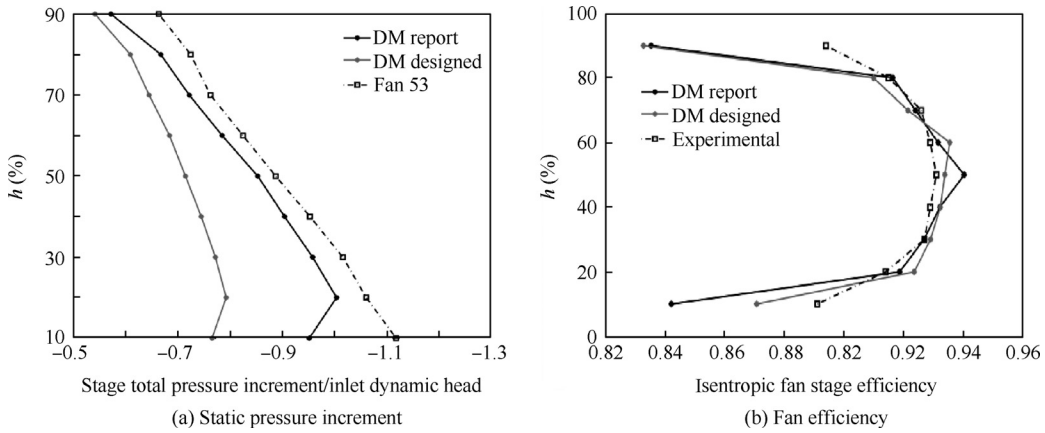

Fig. 10 Meridional fan performance characteristics using discretized Miller approach with blade geometry from Osborn[10] (report) and data from blade design module (designed).

The difference in the axial velocities after the rotor was found to present a similar trend to the circumferential distortion cases assessed with the parallel compressor approach,[22] where the high velocity streams are less accelerated due to the lower pressure increment of these streams. In the parallel compressor approach, this is achieved by the assumption of equality of static pressures between clean and distorted streams at the back of the fan. For the discretized Miller approach is difficult to assume a similar static pressure at the back of the rotor, due to the difference in pressure increment along the blade span, an adaptation was implemented. For the discretized Miller approach, the axial speed at the rotor exit is iterated till the difference between the mean line static pressure of the blade passage operating at the fan top (the highest axial velocities) and bottom (the lowest axial velocities) is less than 2%.

Since in the test case the fan geometry and axial velocities distribution at the exit of the rotor are unknown, the approach which incorporates the blade design module and the aforementioned assumptions has been used in the following analysis. It is opined that for the level of fidelity utilized in this study for the preliminary analysis of BLI systems with TeDP, the loss in accuracy due to the previous assumptions will affect the trends of fan performance under distorted conditions to small extent. This is important as it is more relevant to capture the trend of the phenomena rather than to give accurate performance predictions at preliminary design stage when several configurations need to be tested.

3.2. Distorted case

The results obtained for the case of non-uniform inlet conditions are shown in this section. First, a comparison of the predictions between the discretized Miller and CFD approach is presented. The computational study from Jerez et al.[1] is selected due to the similar circumferential distortion pattern to the test case and the data available for the simulation of the incoming flow. It also presents an experimental validation, which allows the accuracy assessment of the CFD simulation. In the second part, the sample BLI configuration (test case) at design point is examined.

3.2.1. Validation of discretized Miller method for circumferential distortion

The study presented by Jerez et al.[1] examines the NASA axial flow fan stage 67 using CFD and experimental approaches under total pressure distortion covering 1/3rd sector of the inlet flow field. Fig. 11 shows the domain used for the analysis of the fan under distorted conditions examined by Jerez et al.[1] The operating conditions for this analysis are taken according to the study of Jerez et al.[1] and they correspond to 90% of the design speed, corrected mass flow of 32 kg/s based on inlet, mass-averaged stagnation quantities and a DC_{120} of 83%.

To verify the discretized Miller approach, the clean conditions of the single stage NASA axial flow fan stage 67[23] and the distorted conditions studied by Jerez et al.[1] are utilized. The clean conditions in the cases presented in Fig. 12 are assumed to be equal to the undistorted sector of the incoming flow (upper fan or 0°), and the angle measurement takes a different angular position rather than the assumed one in this work. This can be observed in Fig. 5. Due to the fan's ability to impart more energy to the lower momentum flow region, the ratio presented in the aforementioned figure is larger than the one for some radial positions.

The comparison of total pressure increment through the fan assembly predicted by the discretized Miller method and the values reported by Jerez et al.[1] are shown in Fig. 12.

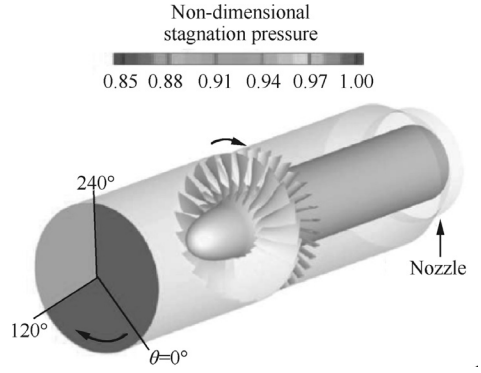

Fig. 11 Isometric view of computational domain.[1]

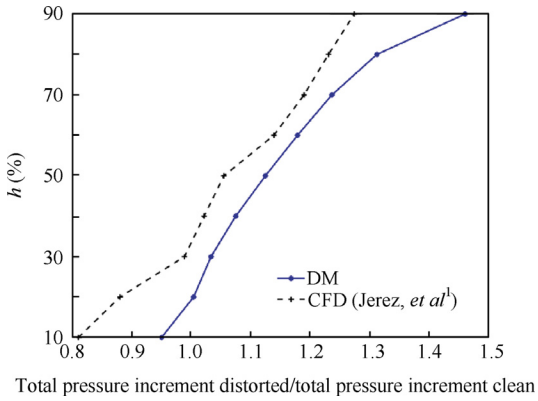

Fig. 12 Total pressure increment along blade span corrected for clean condition. The results from Jerez[1] are included.

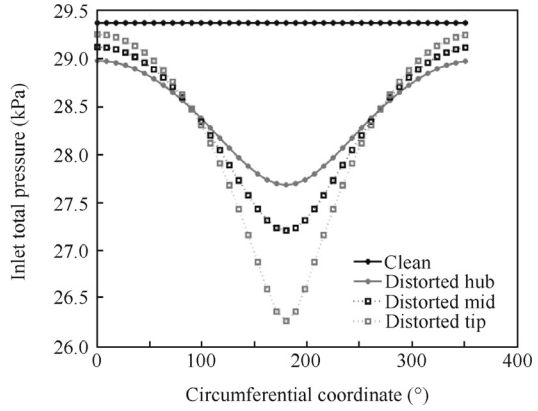

Fig. 13 Inlet total pressure for distorted BLI case.

Fig.12 shows similar trends for the pressure increment values calculated using the discretized Miller and CFD approaches. In this figure, the most distorted blade passage is shown (fan bottom or 180°). The differences in the hub and tip regions are attributed to the limitations of the empirical correlations to predict losses at these stations, and to the small root to tip ratio that the NASA axial flow fan stage 67 presents. Since in the present model the free vortex condition is assumed for the blade design, the small root to tip ratio generates excessive flow deflections, and hence higher losses in these sectors. On the other hand, the offset at the midspan between the values in Fig. 12 is attributed to the assumptions of incompressible flow and constant axial speed through the fan assembly.

Other assumptions which contribute to the discrepancies observed are negligible radial and circumferential interactions and non-separation in regions of high distortion.

These effects are more severe for this case than for the NASA axial flow fan stage 53, as it operates at higher pressure ratios.

To summarize, it is opined that the discretized Miller method captures the trend of the values and hence it could enable the assessment of the detriment in fan performance due to BLI. Further refinement would be recommended to improve the accuracy of the method. However, for the level of fidelity required at the preliminary design stage, the trends of the values for the fan performance characteristics are important to highlight potential benefits/drawbacks in the configuration of BLI systems.[9] The discretized Miller method presents a good balance between accuracy and complexity. The simulation carried out by Jerez et al.[1] for circumferential distortion can illustrate the high computational demanding that assessing BLI induced distortion is for the case of CFD. For instance, in that study the simulation of the total domain (rotor, stator and duct), which has a size of approximately 42.5×10^6 elements, took two months on a 128 CPUs cluster.[1]

3.2.2. Case studied: BLI configuration

Since the aim of the present method is to be implemented in the analysis of TeDP systems with BLI at component and system levels, the BL flow properties can be included in the assessment.

This part of the work assesses the performance of the fan propulsor on the N3-X aircraft concept, operating as a part of the distributed propulsion system with BLI. Some of the characteristics for this case are described in Table 5. For this case, the total pressure distortion in the inlet flow field is developed using the procedure explained in Section 2.3.2. The mass averaged inlet total pressure distortion used for the BLI case is shown in Fig. 13. The meridional performance characteristics at different circumferential positions are shown in Fig. 14 (a) and (b). Fig. 14(c) and (d) shows the mass averaged values for these parameters at different circumferential positions. Table 6 provides the mass averaged values for the fan performance under clean and distorted conditions.

Fig. 14 shows that the pressure increment for the distorted case is larger than that for the clean case. This is attributed to the lower axial velocity that the distorted profile presents. This reduction in axial velocity at the distorted locations (Fig. 5) produces a lower relative velocity at the inlet, which contributes to the increase of the pressure increment through the blade. For this reason, the blade passage located at 180° where the axial velocity is the lowest (according to the distorted profile assumed) presents the highest pressure increment. As expected, in the case of the isentropic efficiency, it is observed that the sectors experiencing lower distortion present higher efficiency due to the lower pressure loss coefficients. Also it is observed that in the tip region for the sectors less distorted 60° the isentropic efficiency is higher than the clean case. This is related to the aforementioned reason, whereas the sectors experiencing lower distortion and relative high pressure increment present less sensitivity to the pressure losses. In the region of high distortion (fan bottom), the pressure losses increase and the efficiency is affected more severely.

The trends of the values for the case of the circumferential fan performance characteristics (Fig. 14(c) and (d)) indicate a greater drop in efficiency in the locations of low velocity, corresponding to what should be expected in BLI systems.[4,1]

The fan performance characteristics for the clean and distorted case are summarized in Table 6. In this table, the values shown correspond to the discretized Miller approach assuming that the propulsor unit delivers the same amount of thrust for the clean and distorted cases. In this table, a 3% drop in mass averaged fan efficiency is obtained and can be attributed to the higher pressure ratio that the distorted case presents in order to match the thrust of the clean case. This produces a reduc-

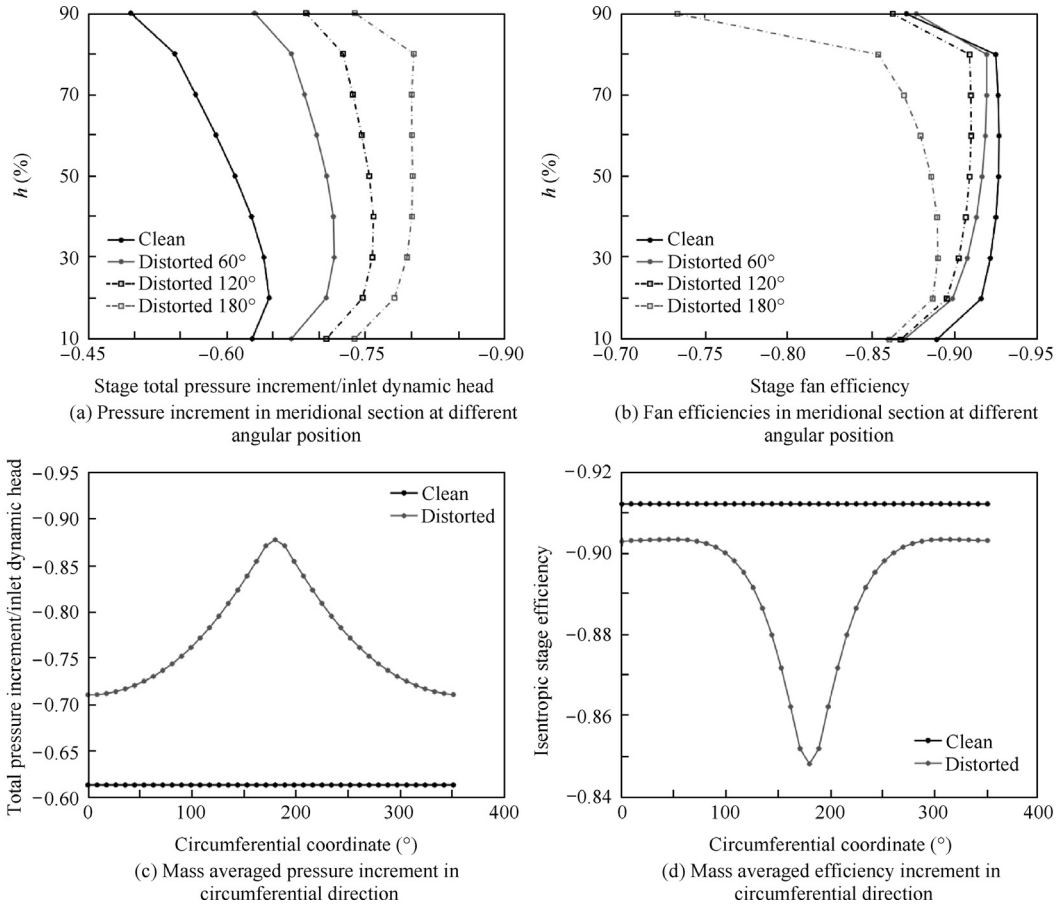

Fig. 14 Meridional and circumferential fan performance characteristics for BLI configuration.

Table 6 Mass averaged fan characteristics for BLI case.

Parameter	Clean	Distorted
Mass flow (kg/s)	55.26	48.84
Stage pressure ratio	1.19	1.25
Isentropic stage efficiency	91.25	88.15

tion in the propulsors' mass flow and consequently reduces the height of the capture sheet, which increases the rate of distortion (the low momentum region of the BL is ingested).[9] The other reason for this large drop in fan efficiency is that neither the duct nor fan have been designed to deal with distortion. Therefore, if better designs for these components are implemented, this large detriment in performance could be reduced. In the work of Florea,[24] an aerodynamic analysis of a tolerant fan to BLI distortion is assessed using CFD. However, the complexity of the flow requires that the layout and detailed geometry for these components are defined. As mentioned before, the purpose of the discretized Miller is to be adaptable for preliminary design and highlight main trends which will be helpful to lead to the detailed design of optimum propulsion architectures with high-fidelity approaches that require more computational resources.

4. Conclusions

This work highlights the computational and time limitations that CFD methods present for distortion problems in BLI systems. Furthermore, this work presents an alternative method that is computationally cheap based on well-known empirical correlations and mean-line design, which has the novelty of discretizing the inlet region in circumferential and radial streams, so that the combined distortion patterns that BLI presents can be assessed. For this method, which denominates the discretized Miller approach, a set of empirical correlations to predict loss coefficients at different blade span locations have been determined. This tool shows good agreement for cases considering uniform and distorted flow, and further due to its simplicity, it can be considered suitable for preliminary design of BLI systems at design point. The application of the discretized Miller approach enables assessment of the effects of BLI in a propulsor fan. The approach indicates that BLI may result in a decrease of 3% in fan efficiency for the configuration studied. Such deterioration in fan performance will consequently lead to an increase in TSFC and hence fuel burn. This will then necessitate redefinition of previously generated optimal (distributed propulsion) configurations. The suitability of new BLI propulsion architectures then could also be assessed by incorporating the tool developed in this work, and hence the effects of combined radial and circumferential

distortion can be included in the performance calculation at component and system levels.

In addition, the method presented here is aimed at undertaking preliminary design of distributed propulsion systems with BLI and hence the simplifications utilized are at the expense of accuracy. Some of the modifications which could be implemented to improve the accuracy of the presented method are as follows:

(1) Improve the pitch to chord ratio rule[25], so that it will better match experimental values.
(2) Improve the blade design code using more accurate blade design theories such as exponential blading.
(3) Refine the sectors close to the tip and hub regions using a non-uniform discretization; however this will require further improvement of the actual empirical correlations so as to improve the accuracy of predictions in these sectors.
(4) Require to take into account the compressibility effects while calculating the pressure increments over the flow. This is an important aspect to consider as these effects become more noticeable in fans operating at high pressure ratios.
(5) The assumption of constant axial speed through the fan assembly could also be avoided.

Acknowledgement

The authors gratefully acknowledge the financial support provided by Escuela Politecnica Nacional for the development of the project PIMI 15-03 and PIJ 15-11. They also thank Cranfield Departamental Grant for the support provided.

References

1. Jerez V, Hall C, Colin Y. A study of fan distortion interaction within the NASA rotor 67 transonic stag. *J Tomach* 2012;**134**(5), 051011-1–051011-12.
2. Cirligeanu R, Pachidis V. *IGV loss and deviation modelling* [dissertation]. Cranfield: Cranfield University; 2010.
3. Plas A. *Performance of a boundary layer ingesting propulsion system* [dissertation]. Massachusetts: Massachusetts Institute of Technology; 2006.
4. Doulgeris G. *Modelling and integration of advanced propulsion systems* [dissertation]. Cranfield: Cranfield University; 2008.
5. Pachidis V, Pilidis P, Templalexis I, Marinai L. An iterative method for blade profile loss model adaptation using streamline curvature. *J Eng Gas Turb Power* 2008;**130**(1), 011702-1–011702-8.
6. Redmond J. *Effect of BLI-Type inlet distortion on turbofan engine performance* [dissertation]. Blacksburg, VA: Virginia Polytechnic Institute and State University; 2013.
7. Felder J, Dae Kim H, Brown, G. Turboelectric distributed propulsion engine cycle analysis for hybrid-wingbody aircraft. In: *Proceedings of the 47th AIAA aerospace sciences meeting including the new horizons forum and aerospace exposition*; 2009 January 5–8; Florida, USA; 2009.
8. Florea R, Stucky M, Shabbir A. Parametric analysis and design for embedded engine inlets. *J Propul Power* 2015;**31**(3):843–50.
9. Valencia E, Nalianda D, Laskaridis P, Singh R. Methodology to assess the performance of an aircraft concept with distributed propulsion and boundary layer ingestion using a parametric approach. *J Aerospace Eng* 2015;**229**(4):682–93.
10. Osborn W, Moore R, Steinke R. Aerodynamic performance of a 1.35-pressure ratio axial-flow fan stage, Washington D.C.: NASA; 1978. NASA Technical Paper Report No.: 1299.
11. Felder J, Dae Kim H, Brown G. An examination of the effect of boundary layer ingestion on turboelectric distributed propulsion systems. *Proceedings of the 49th AIAA Aerospace Sciences Meeting including the New Horizons Forum and Aerospace Exposition*; 2011 Jan 4-7; Florida, USA. Reston: AIAA; 2011.
12. Plas AP, Sargeant MA, Madani V, Crichton D, Greitzer EM, Hynes TP, et al. Performance of a boundary layer ingesting (BLI) propulsion system. *Proceedings of the 45th AIAA aerospace sciences meeting and exhibit*; 2007 Jan 8-11; Nevada. Reston: AIAA, 2007.
13. Saravanamuttoo H, Rogers G, Cohen H. *Gas turbine theory*. 5th ed. Harlow: Prentice Hall; 2001.
14. Miller D, Wasdell D. *Off-design prediction of compressor blade losses*. IMECHE C279/87; 1987.
15. Howell A. Fluid dynamics of axial compressors. *Proceedings of the institution of mechanical engineers, development of the internal combustion turbine*; 1945. p. 441–52.
16. White N, Tourlidakis A, Elder R. Axial compressor performance modelling with a quasi-onedimensional approach. *Proc Inst Mech Eng, Part A: J Power Energy* 2002;**216**(2):181–93.
17. Wright P, Miller D. An improved compressor performance prediction model. In: *Turbomachinery latest development in a changing scene. Proceedings of the IME European conference*; 1991 March. p. 19–20.
18. Schwenk F, Lewis G. *A preliminary analysis of the magnitude of shock losses in transonic compressors*. Washington, D.C. (WA): Research Memorandum, National Advisory Committee for Aeronautics; 1957. No. NACARM E57A30.
19. Howell A, Bonham R. Overall and stage characteristics of axial-flow compressors. *Proceedings of the institution of mechanical engineers* 1950; 1950 June.
20. ANSYS Release 15. *ANSYS CFX-solver modelling guide*. ANSYS; 2013.
21. Sun Zhenyu, Singh Riti, Laskaridis Panagiotis. *CFD analysis of boundary layer ingestion propulsion* [dissertation]. Cranfield: Cranfield University; 2013.
22. Liu C, Singh R, Laskaridis P, Doulgeris G. *Turboelectric distributed propulsion system modelling* [dissertation]. Cranfield: Cranfield University; 2013.
23. Cunnan W, Stevans W, Urasek D. *Design and performance of a 427-meter-persecond-tip-speed two-stage fan having a 2.40 pressure ratio*. Washington, D.C.: NASA; 1978. Technical Paper Report No.: 1314.
24. Florea R, Voytovych D, Tillman G, Stucky M, Shabbir A, Sharma O, et al. Aerodynamic analysis of a boundary-layer-ingesting distortion-tolerant fan. *Proceedings of the American Society of Mechanical Engineers; ASME*; 2013 June 3–7. Texas: Solar Turbines Incorporated; 2013.
25. Carter ADS. *The low speed performance of related airfoils in cascade*. London: Majesty's Stationery Office; 1949. Report No. R55.

Esteban Valencia is an associate professor at Mechanical Engineering School, Escuela Politecnica Nacional of Ecuador (EPN). Currently, he is a lecturer of fluid mechanics and thermodynamics of turbomachinery. He is also head of the Turbomachinery and Fluid Mechanics Laboratory. His research involves the design of innovative propulsion architectures for aerial systems. He received his Ph.D. degree from Power and Propulsion Department, Cranfield University, UK.

Victor Hidalgo received the B.S. degree in Mechanical Engineering from Escuela Politécnica Nacional (EPN), Quito in 2008, the M.S. degree in fluid mechanics from China University of Mining and Technology, Xuzhou in 2012, and the Ph.D. degree in power engineering and Eng. thermal physics from Tsinghua University, Beijing in

2016. Presently, he is an associate professor in mechanical engineering at EPN, Quito.

Devaiah Nalianda received the Ph.D. degree in techno-economic environmental risk assessment from Cranfield University in 2012 and the M.S. degree in thermal power (gas turbine technology) from Cranfield University in 2009. Devaiah's research is focused on conceptual development and application of distributed propulsion systems for civil aircraft.

Laskaridis Panagiotis received the B.E. degree in aerospace systems engineering from Coventry University, the M.S. degree in aerospace vehicle design from Cranfield University and the Ph.D. degree in performance evaluation and systems integration for more electric aircraft from Cranfield University. During his Ph.D. student period, he worked closely with Goodrich Corporation on the subjects of all/more electric aircraft as well as use of an electric motor to drive an afterburner pump.

Riti Singh is an emeritus professor of Cranfield University. He leads the Gas Turbine Engineering and Technology Group within the Department of Power and Propulsion and is the director of the Rolls-Royce University Technology Centre in Performance Engineering. He was previously deputy head of School of Engineering and head of Department of Power, Propulsion and Aerospace Engineering.

Cranfield University

CERES https://dspace.lib.cranfield.ac.uk

School of Aerospace, Transport and Manufacturing (SATM) Staff publications (SATM)

2016-12-21

Discretized Miller approach to assess effects on boundary layer ingestion induced distortion

Valencia, Esteban

Elsevier

Valencia E, Hidalgo V, Nalianda D, et al., (2017) Discretized Miller approach to assess effects on boundary layer ingestion induced distortion. Chinese Journal of Aeronautics, Volume 30, Issue 1, February 2017, pp. 235-248

http://dx.doi.org/10.1016/j.cja.2016.12.005

Downloaded from Cranfield Library Services E-Repository